MIT Open Access Articles

Design of conditions for self-replication

Massachusetts Institute of Technology

Design of conditions for self-replication

Sumantra Sarkar[*] and Jeremy L. England[†]

Physics of Living Systems, Massachusetts Institute of Technology, 400 Technology Square, Cambridge, Massachusetts 02139, USA

A "self-replicator" is usually understood to be an object of definite form that promotes the conversion of materials in its environment into a nearly identical copy of itself. The challenge of engineering novel, micro- or nanoscale self-replicators has attracted keen interest in recent years, both because exponential amplification is an attractive method for generating high yields of specific products and, also, because self-reproducing entities have the potential to be optimized or adapted through rounds of iterative selection. Substantial steps forward have been achieved both in the engineering of particular self-replicating molecules and in the characterization of the physical basis for possible mechanisms of self-replication. At present, however, there is a need for a theoretical treatment of what physical conditions are most conducive to the emergence of novel self-replicating structures from a reservoir of building blocks on a desired time scale. Here we report progress in addressing this need. By analyzing the kinetics of a toy chemical model, we demonstrate that the emergence of self-replication can be controlled by coarse, tunable features of the chemical system, such as the fraction of fast reactions and the width of the rate constant distribution. We also find that the typical mechanism is dominated by the cooperation of multiple interconnected reaction cycles as opposed to a single isolated cycle. The quantitative treatment presented here may prove useful for designing novel self-replicating chemical systems.

I. INTRODUCTION

The emergence of self-replicators from a mixture of components is marked by exponential growth of one or more multicomponent structures. This process is of great practical importance due to the possibility of exponentially rapid synthesis of target structures and, also, has previously been considered in models of prebiotic chemistry [1–5]. The mechanisms that enable self-replication in a soup of metastable bound states have been investigated intensively in the past decades [6,7] and continue to inspire new attempts [8–17]. The processes of self-replication described in these studies, though distinct, share two mechanistic elements: (a) the existence of at least one autocatalytic cycle (ACC) and (b) a source of driving that runs the autocatalytic cycle.

In the usual case [6] an autocatalytic cycle is designed by experimenters to consume one or more building blocks that are provided in excess to generate replicas of a template that is used as a seed. A significant challenge in any such case lies in devising an appropriate chemical library that limits parasitic side reactions. Theoretical approaches, meanwhile, have been most successful in the opposite regime, where the catalytic network is sufficiently densely connected, and every molecule available in the reaction pot catalyzes the production of at least one other molecule [18–20]. In this case, it is possible to formulate general criteria for the onset of positive feedback loops in the catalytic reaction network

that lead to the exponential growth of the molecules in these loops. Thus, although it is qualitatively understood that robust self-replication requires sufficient catalytic promiscuity that somehow avoids excessive side reactions, there is need for a quantitative treatment of this trade-off in a physical model that may provide future guidance for the design of conditions conducive to the spontaneous emergence of self-replicators from customizable mixtures of nano- or microscale components [21,22]. Therefore, we sought to investigate a toy model where all possible stoichiometric combinations of certain building blocks are considered in the construction of an effective model of a "chemical" space. Using this model (Fig. 1 and Appendix A), we lay out general conditions for the emergence of exponential growth in systems without explicit catalysis. Interestingly, we find that the typical mechanism for the emergence of self-replicators occurs via a multicycle topological element in the reaction and, therefore, violates previously established quantitative criteria for self-replication that were developed assuming that self-replication occurs through isolated autocatalytic cycles [4,5].

II. MODEL

A. Toy chemical system

We undertook to model a large, well-mixed reaction pot with diverse possible combinations of monomers. We call these monomers "atoms" here because we eventually plan to model the dynamics of their bound states using thermodynamically consistent mass-action kinetics, but it should not be imagined that we intend exclusively or even principally to describe real molecular chemistry using the model presented here. Rather, the essence of the "chemical space" constructed
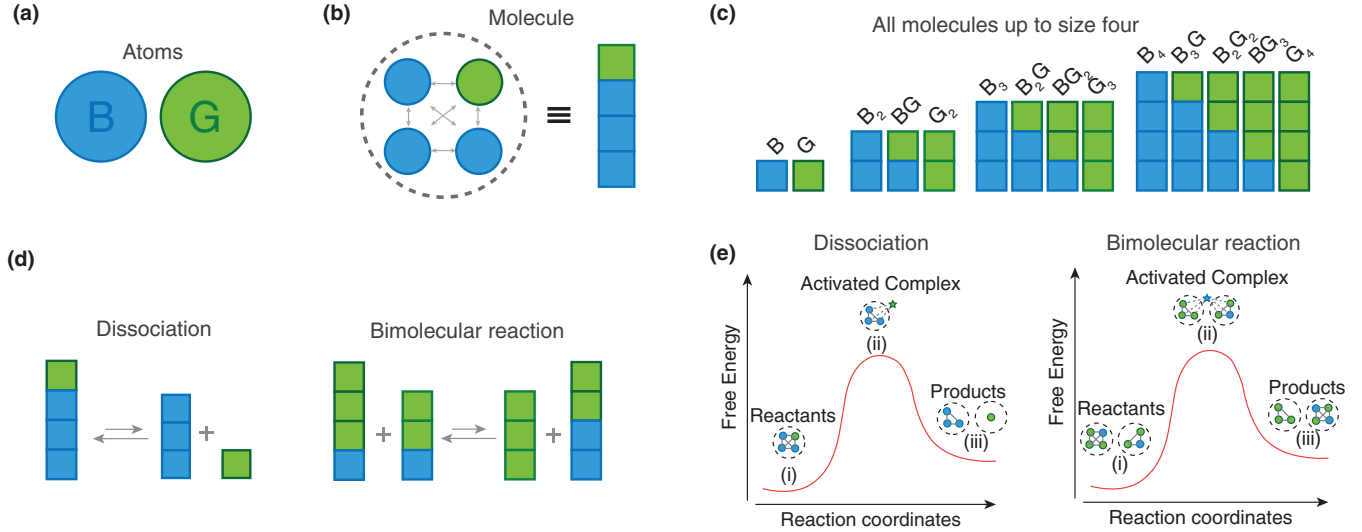
FIG. 1. Toy chemical system with two monomer types. (a) The toy chemical system (see Appendix A) consists of two *atoms*, *B* and *G*. (b) The atoms interact with each other at three interaction energies, ϵ_{BB}, ϵ_{BG}, and ϵ_{GG} (measured in units of kT), to form *molecules*, which are represented as a stack of atoms. ϵ_{XY} denotes the interaction energy between an atom of type X and another atom of type Y. Gray arrows represent interactions between different atoms. All atoms inside a molecule, such as the one shown here, interact with each other. (c) The current model consists of 14 molecules that contains at most four atoms. (d) The molecules take part in dissociation or bimolecular reactions. (e) In the mechanistic model (see Appendix A), the rate constants of these reactions are calculated from a transition-state model. Star-shaped atoms are atoms that are being donated. Circular atoms are other atoms in the molecules.

is that it is a vast space of diverse combinations among physical interacting components such as polymer-coated colloidal particles or DNA origami [Fig. 1(a)].

In our model, two or more atoms interact with each other to form a bound state, which we call a "molecule." For simplicity, we assume that the molecules do not have any internal structure and all the atoms inside a molecule interact with all other atoms in that molecule with interaction energy ϵ_{BB}, ϵ_{BG}, or ϵ_{GG} [Fig. 1(b)]. Since the molecules do not have any internal structure, their free energies are completely determined by their composition and the three ϵ parameters. Also, we assume that each molecule contains at most $\mu_{\max}$ atoms and forbid all other bound states. Except where it is explicitly mentioned, we set $\mu_{\max} = 4$. With these two assumptions it can be shown that there are 14 distinct molecules in the model with two types of monomers [Fig. 1(c)].

The molecules take part in reactions that involve one molecule donating an atom to the surrounding medium or to another molecule. We call the former a dissociation reaction and the latter a bimolecular reaction [Fig. 1(d)]. The reactions are activated processes and the rate constant of a given reaction that takes the reactant state i to product state j is inversely proportional to the exponential of the barrier height: $k_{ij} \propto \exp(-B_{ij})$. The activation barriers B_{ij} are chosen either randomly or using a model of the transition state. We refer to the latter as the *mechanistic model*.

In the mechanistic model, $B_{ij} = F_{ij}^{\mathrm{Tr}} - F_i$, where F_i is the free energy of the reactant state and F_{ij}^{Tr} is the free energy of the transition state. F_i is determined from the interaction energies. To calculate F_{ij}^{Tr}, we assume that during a reaction, the donated atom first goes to an excited state, where it interacts with other atoms in the donor molecule through a weakly repulsive interaction [Fig. 1(e)] that is proportional to the ground-state interaction energy. The proportionality factor

$c_0 = -0.1$ is the same for all three interaction energies and is a parameter of the model. The results described are robust to variation in c_0, as long as $\epsilon_{BB,BG,GG} < 0$ and $c_0 < 0$.

The resulting toy "chemistry" generates a full system of rate equations with mass-action kinetics governing the concentrations of different allowed molecules. There is no explicit catalysis or autocatalysis in this system at the level of a single reaction, but catalytic and autocatalytic cycles appear naturally in the reaction network (defined in the next section) due to coupling between different reactions. In what follows, we explicitly solve this set of equations in two instances of the model with one and two types of atoms. We investigate the resultant transient kinetics of the molecular concentration to identify the conditions necessary for the persistence of one or more autocatalytic cycles that drive the exponential growth of a subset of the molecules.

B. Reaction network

1. Coupled-reaction graph

In our model, the products of various reactions act as reactants to other reactions. For example, in the following two reactions one of the products of **r1**, B, is used as a reactant in **r2**:

$$\mathbf{r1}: \quad BG + B_2 \rightarrow B + B_2G, \tag{1}$$

$$\mathbf{r2}: \quad B + B_2 \rightarrow B_3. \tag{2}$$
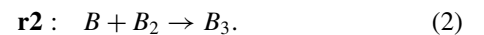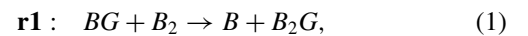
Hence, **r1** is coupled to **r2**. We graphically represent this relationship by constructing a directed graph whose nodes are reactions **r1** and **r2** and which has a directed edge from **r1** to **r2** [Fig. 2(a)]. A graphical representation of all 180 reactions in our model is shown in Fig. 2(b). Three reaction motifs
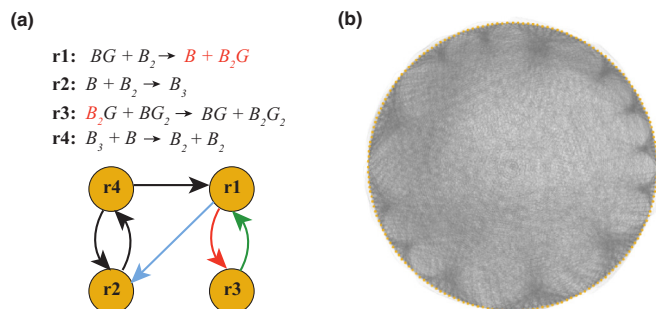
(a)

r1: $BG + B_2 \rightarrow B + B_2G$
r2: $B + B_2 \rightarrow B_3$
r3: $B_2G + BG_2 \rightarrow BG + B_2G_2$
r4: $B_3 + B \rightarrow B_2 + B_2$

(b)

FIG. 2. Reaction network. (a) Definition of the reaction network: The reactions are the nodes of this network and a directed edge from node **ri** to node **rj** exists if any of the products of reaction i are used as the reactant in reaction j. For example, in the example considered here, **r1** produces B and B_2G, which are used as reactants in **r2** and **r3**, respectively. Hence, as shown, in the reaction network there are directed edges from **r1** to **r2** and **r3**. Similarly, BG is a product of **r3**, which is used as a reactant in **r1**. Hence, there is a directed edge from **r3** to **r1**. (b) Generic structure of the reaction network of our model.

are usually found in the reaction network: catalytic cycles, autocatalytic cycles, and lossy side reactions.

2. Network motifs

a. Catalytic cycles (CCs). Consider reactions **r1** and **r3** in Fig. 2(a). Both of them have a directed edge from one to the other. Hence, if by some process **r1** and **r3** run in sequence for some time, then the net output will be the production of B and B_2G_2 from B_2 and BG_2, catalyzed by BG and B_2G. It is easy to show that other cycles, such as **r1** $\rightarrow$ **r2** $\rightarrow$ **r4** $\rightarrow$ **r1** and **r2** $\rightarrow$ **r4** $\rightarrow$ **r2**, are also catalytic cycles. In fact, any cycle in the reaction graph defined here is a catalytic cycle.

b. Autocatalytic cycles (ACCs). A subset of the catalytic cycles has the special property that at least one of the catalyst molecules is produced in excess. That is, the catalyst molecule catalyzes its own production. We refer to such cycles as autocatalytic cycles. For example, it is easy to see that **r2** $\rightarrow$ **r4** $\rightarrow$ **r2** is an autocatalytic cycle, because B_2 catalyzes its own production.

c. Lossy side reactions. In a complex reaction network, such as ours, it is likely that reactions are coupled to more than one reaction. Therefore, quite often, the function of an autocatalytic cycle is hindered by the presence of parasitic side reactions that couple to one of the reactions in the autocatalytic cycle and usurp the resources required to drive the cycle. For example, **r1** is a lossy side reaction for the autocatalytic cycle **r2** $\rightarrow$ **r4** $\rightarrow$ **r2**. As shown in Fig. 2(a), lossy reactions need not be an isolated reaction. Often, they are part of another catalytic or autocatalytic cycle. When it is part of another autocatalytic cycle, the parasitism is equivalent to competition between two autocatalytic cycles.
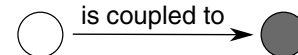
III. CONDITIONS FOR SELF-REPLICATION

The physicochemical conditions required for self-replication are very different in an interacting chemical system, such as ours, than in isolated autocatalytic cycles, which have been studied theoretically and experimentally
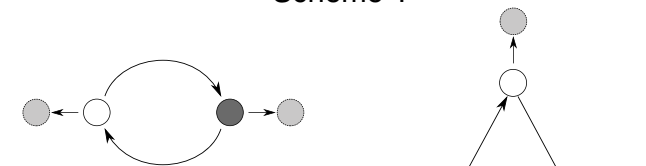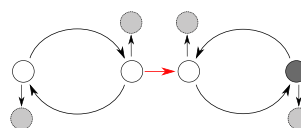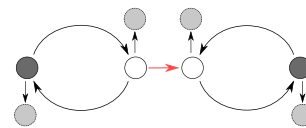
Reaction internal to cycle
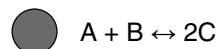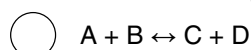
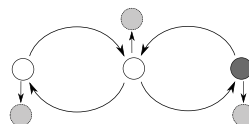$A + B \leftrightarrow C + D$

$A + B \leftrightarrow 2C$

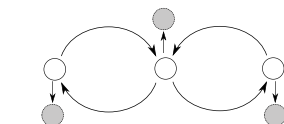Reaction external to cycle

is coupled to

FIG. 3. Modes of self-replication. Open circles represent reactions of type $A + B \leftrightarrow C + D$; dark circles, reactions of type $A + B \leftrightarrow 2C$. To remain consistent with the definition of coupled reactions, we consider that the reverse reaction of a reaction is not coupled to the reaction. Scheme 1: Isolated autocatalytic cycles (ACCs). On the left is a two-step ACC and on the right is a three-step ACC. A two-step ACC can be constructed from the following two reactions. Open circle, $BG + B_2 \rightarrow B_3 + G$; dark circle, $B_3 + B \rightarrow 2B_2$. Scheme 2: A catalytic cycle (CC) is coupled to an ACC through the waste product of the former (red arrow). Scheme 3: An ACC is coupled to another ACC through the waste of the former. Scheme 4: A CC is coupled to an ACC through a catalyst, which is also a catalyst for the ACC. Scheme 5: A CC is coupled to another CC by the sharing of a catalyst molecule between them. In all of these schemes the light-gray reactions are reactions that couple to the reactions in a motif but are not part of it.

over the last few decades. Prior work has indicated that the kinetic dominance of reactions can be quantified through a measure called specificity. It has been shown that for any cycle, the product of the specificity, which we call cycle specificity for the sake of brevity, has to be greater than 0.5 for a reaction cycle to run. However, this result is incomplete. As we show here, even for an isolated autocatalytic cycle, other conditions have to be met for self-replication to take place. Furthermore, self-replication in an interacting system can happen even when the cycle specificity of all the autocatalytic cycles is orders of magnitude less than 0.5, requiring a fresh search for the conditions required for self-replication.

To establish these conditions, we study the kinetics of simple network motifs that are outlined in Fig. 3. This is

TABLE I. Conditions for self-replication for schemes 4 and 5. Values tabulated are the numerically obtained minimum specificity required for the concentration to grow exponentially. The minimum value numerically investigated is 0.0001. Therefore, it is possible that for entries with a tabulated value of 0.0001, the minimum specificity required may be less than 0.0001. One should note that the established criteria [4,5] would predict that self-replication is not possible when specificities are this low. This table clearly demonstrates the limitation of the previous criteria. σ_1 is the specificity of the reaction that is shared by both cycles. $\sigma_{2,3}$ are the other reactions in the scheme. Particularly for scheme 4, σ_3 denotes the specificity of the doubling reaction (dark circle in Fig. 3).

σ_1	σ_2		σ_3	
	Scheme 4	Scheme 5	Scheme 4	Scheme 5
0.1	0.8418	0.9180	0.8154	0.9180
0.2	0.7356	0.8542	0.6142	0.8294
0.3	0.6573	0.7780	0.4422	0.7443
0.4	0.5693	0.7356	0.2130	0.6487
0.5	0.5232	0.6817	0.0318	0.5509
0.6	0.4768	0.6573	0.0001	0.4409
0.7	0.4307	0.6142	0.0001	0.3427
0.8	0.4007	0.5693	0.0001	0.2413
0.9	0.3858	0.5693	0.0001	0.1241
1.0	0.3427	0.5232	0.0001	0.0002

by no means an exhaustive list of network motifs that lead to self-replication, but these are the simplest ones to study. We summarize the necessary conditions for self-replication for these motifs below. The derivation of these conditions is described in Appendix B. The sufficient condition for self-replication is the union of all the necessary conditions.

a. Scheme 1: Isolated ACCs. For isolated ACCs, the cycle specificity has to be greater than 0.5, in agreement with previous results. However, additionally, the chemical current (see Appendix A for the definition) for all the reactions has to be greater than 0 and an increasing function of time.

b. Schemes 2 and 3: For scheme 2, no exponential growth occurs unless the specificity of the ACC is greater than 0.5. For scheme 3, it is possible to observe exponential growth as long as one of the ACCs has a specificity greater than 0.5.

c. Schemes 4 and 5: It is difficult to write a simple closed expression for the condition required for exponential growth. However, under these two schemes, it is possible to observe exponential growth even when both cycles have a specificity less than 0.5. The specificity distribution required for these two schemes is listed in Table I.

IV. COARSE CONTROL OF EXPONENTIAL GROWTH

The fundamental goal of this paper is to clarify how these reaction motifs come to dominate the kinetics and give rise to different types of concentration growth. For example, if the kinetics is dominated by autocatalytic cycles, we expect to observe exponential growth, whereas if the kinetics is dominated by uncoupled reactions, then we expect linear growth. It is to be noted that growth is a strictly transient behavior of the underlying rate equations, which is governed by the topology of the coupled-reaction graph and the instantaneous

rates of the reactions. Therefore, through a suitable choice of the reaction library, which determines the topology, and rate constants, which determine the instantaneous rates, it is possible to manipulate the influence of various motifs on the reaction kinetics.

These facts are well known and have been used qualitatively to design small chemical systems that permit near-exponential growth of molecular concentrations [6]. However, such qualitative knowledge is of little use when large chemical systems with hundreds, if not thousands, of reactions need to be designed for self-replication. To design a chemical network of such complexity, a quantitative relationship between the rate constants and the transient behavior of the reaction network needs to be established. Unfortunately, it is impractical to explore the parameter space of the rate constants to establish such a relationship due to the cost involved in exploring the parameter space, which may be thousand-dimensional. We therefore need to establish the required quantitative behavior using coarse (macroscopic or hydrodynamic) features of the rate constants, for example, in increasing order of coarseness: (a) protocol PF, the fraction of fast reactions; (b) protocol CD, the width of the rate constant distribution; and (c) protocol IE, the interaction energies between the atoms. Due to our interest in self-replication, we focus only on the emergence of exponential growth and establish quantitative criteria using these parameters.

A. PF: Fraction of fast reactions

The most theoretically accessible case arises when all the interaction energies are 0 and the rate constants are chosen in such a way that a controllable fraction, p_{fast}, of the reactions may occur, and the rest are effectively forbidden. To implement this system, we identified the set of all reactions permitted by stoichiometry and drew the random barriers for the reactions from the binary set $\{0, \infty\}$, corresponding to rate constants of 1 or 0. The fast reactions, with rate constants 1, were assigned a probability p_{fast}. To ensure detailed balance conditions, the barriers for the forward and the reverse reactions were set to be equal. As we discuss later in this section, p_{fast} can be mapped to the dispersion of the rate constant distribution, with $p_{\text{fast}} \approx 1$ corresponding to narrow and $p_{\text{fast}} \approx 0$ to broad distributions.

Under these assumptions, the probability of self-replication, p_{sr}, can be estimated (Appendix C) as a function of p_{fast}. Self-replication occurs if and only if at least one autocatalytic cycle in the reaction network has direct and exclusive access to its fuel [Fig. 4(a)]. Hence, p_{sr} can be calculated from (a) the probability of finding at least one autocatalytic cycle with direct access to its fuel, p_{acc} (p_{fast}), and (b) the probability that all autocatalytic cycles have side reactions, p_{loss} (p_{fast}). Hence, for $p_{\text{fast}} = x$,

$$p_{\text{sr}}(x) = p_{\text{acc}}(x) \times (1 - p_{\text{loss}}(x)). \quad (3)$$

As Figs. 4(a) and 4(b) show, self-replication generally sets in spontaneously when a reaction network has a specific level of complexity dictated by the trade-off of the two competing percolation transitions, p_{acc} and p_{loss}—the first of which determines whether there are enough fast reactions to ensure the existence of at least one driven autocatalytic cycle and the
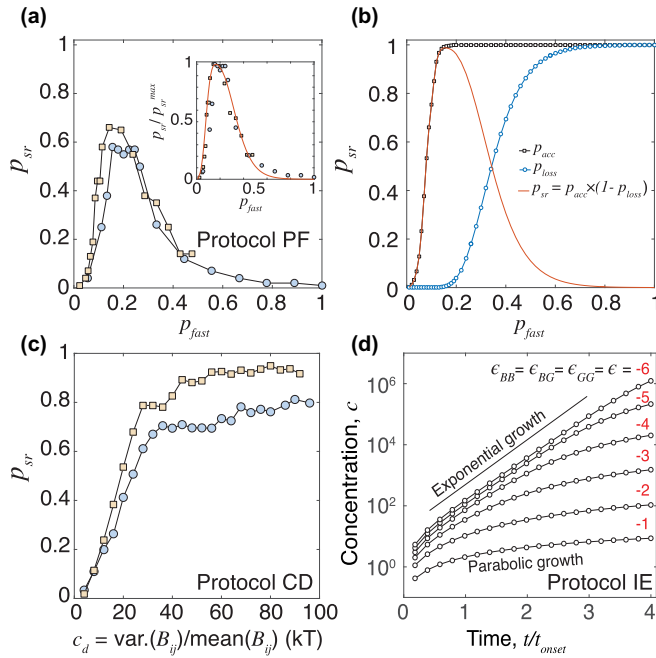
FIG. 4. Coarse control of exponential growth. (a) Protocol PF: Numerical solution of the rate equations shows that the probability of self-replication, p_{sr}, is maximum for an intermediate value of the fraction of fast reactions, p_{fast}. Results are shown for $\mu_{max} = 4$ (blue circles) and $\mu_{max} = 5$ (orange squares), where μ_{max} is the maximum allowed size of the molecules. Inset: Analytical prediction of p_{sr} (shown in B) normalized by its maximum value vs p_{fast} (orange curve) matches well with numerical data. (b) Probability of finding a fueled autocatalytic cycle, p_{acc} (gray squares), and probability of loss of fuel due to side reaction, p_{loss} (blue circles), as a function of the probability of fast reactions, p_{fast}. The probability of self-replication, $p_{sr} = p_{acc} \times (1 - p_{loss})$, is plotted by the orange line. (c) Protocol CD: p_{sr} vs the coefficient of dispersion (variance/mean) of the distribution of activation barriers, B_{ij}, for $\mu_{max} = 4$, $t_{obs} = \infty$ (blue circles) and $\mu_{max} = 5$, $t_{obs} = \infty$ (orange squares). For a narrow distribution ($< 10\,\text{kT}$), no exponential growth is observed and only power-law growth is observed. For a broader distribution ($> 10\,\text{kT}$), p_{sr} increases and eventually saturates with the dispersion of the activation barriers. (d) Protocol IE: As the magnitude of the interaction energy increases, the concentration tends to grow exponentially. For example, for $\epsilon_{BB,BG,GG} = -1$, parabolic growth is observed. However, for $\epsilon BB, BG, GG = -6$, exponential growth is observed.

second of which determines whether reactions are so promiscuously coupled that every cycle is drained by numerous side reactions. Due to this trade-off, an optimal p_{fast} exists at which p_{sr} is maximized. Simply stated, this result implies that emergent self-replication occurs at a high probability when there are enough autocatalytic cycles and no parasitic reactions: a result that is qualitatively well known [6] and perhaps unsurprising. More surprisingly, however, our quantitative treatment shows that this optimality depends only on the reaction network topology (through p_{fast} and the randomized graph connectivity) and should be relatively insensitive to the specific rate constant distribution. Therefore, as long as p_{fast} can be tuned to its optimal value, exponential growth will emerge in a large network with certainty. *What remains now is*
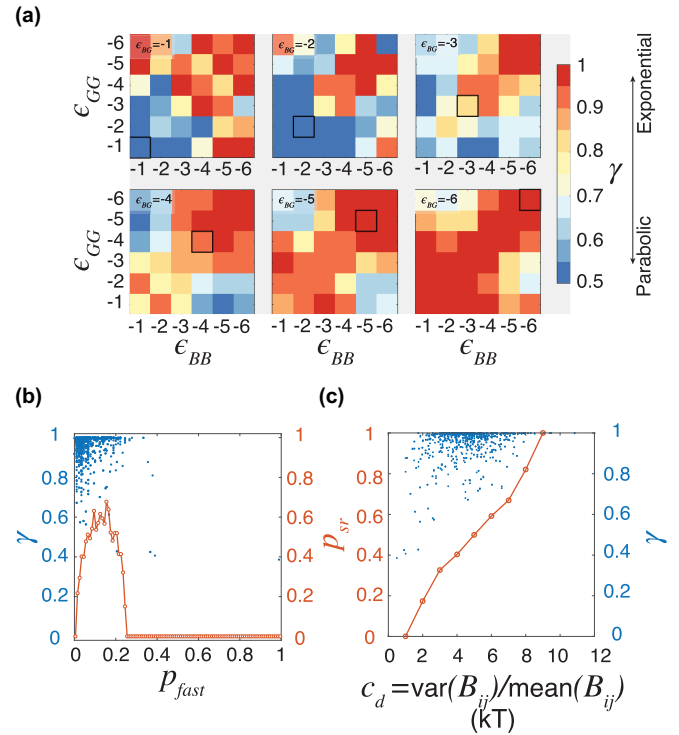

FIG. 5. Protocol IE. (a) Growth exponent γ for different combinations of interaction energies. Red areas correspond to $\gamma = 1$ (exponential growth) and blue areas correspond to $\gamma = 0.5$ (parabolic growth). (b) γ as a function of an estimate of the fraction of the fast reaction (see Appendix A), p_{fast}. The probability of self-replication p_{sr} is defined as the probability of finding $\gamma > 0.99$ and it is non-monotonic with respect to p_{fast}. (c) p_{sr} as a function of the coefficient of dispersion, c_d. The similarity of the results for protocol IE to those for protocols PF and CD indicates equivalence between these three protocols.

to determine whether a quasirandomly connected network is a suitable approximation to a real chemical network and, if so, how we may then tune the effective value of p_{fast} to its optimal value.

B. CD: Width of the rate constant distribution

The first and simplest hypothesis is that the p_{fast} can be tuned to optimality by the dispersion of the rate constants. To demonstrate this, we chose the activation barriers from exponential distributions with varying values of the coefficient of dispersion (variance/mean), c_d, while keeping the interaction energy 0. In the first set of studies, we numerically solved the equations until the concentrations reached steady state ($t_{obs} = \infty$). From the obtained time series of molecular concentrations, we found their growth exponent γ (Appendix A). If $\gamma = 1$, the corresponding concentration grows exponentially. If $\gamma < 1$, the concentration grows subexponentially. The probability of exponential growth, p_{sr}, was determined by finding $\text{Prob}(\gamma > 0.99)$. Under this protocol, when the distribution was too narrow [$c_d < 10\,\text{kT}$ in Fig. 4(c)], the molecules never grew exponentially. However, when the distribution was broader, the probability of exponential growth, p_{sr}, increased
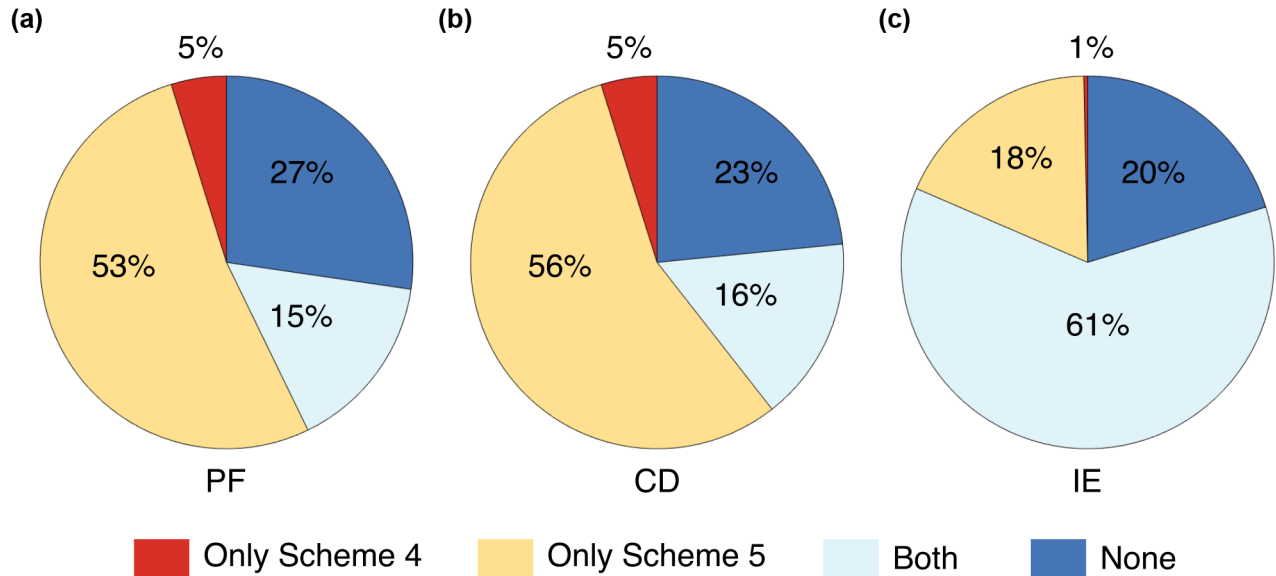
FIG. 6. Pie chart showing modes of self-replication in three protocols: (a) PF, (b) CD, and (c) IE. Isolated ACCs (schemes 1–3) are absent in all three protocols, and surprisingly, the dominant mode of self-replication is scheme 5, which contains no isolated ACC. Where no modes of self-replication are registered, it is likely that self-replication occurs through other motifs that we have not considered here.

with c_d, eventually saturating at a value that is dependent on the underlying reaction network [Fig. 4(c)].

C. IE: Interaction energy

In most experiments, it is easier to control the interaction energies of the building blocks (atoms) than the rate constant distribution of the generated reaction network. Therefore, our theoretical results will be useful if and only if it can be established that the simplifying assumption of quasirandom chemical network connectivity is effectively valid for more realistic models in which reaction rate kinetics are determined by underlying physical quantities such as interaction energies between components. We therefore sought next to analyze a "mechanistic model" in which the activation barriers of the reactions are obtained by assuming a transition-state model of the reaction kinetics [Fig. 1(e)]. The energies of the ground and the transition states are determined by the interaction energies of the atoms, which are allowed to form clusters of up to four members. Therefore, the dispersion of the rate constants can be controlled by changing the interaction energies. Typically, stronger interaction energies correspond to broader distributions of rate constants. Hence, as per our results from protocol CD, we expect to observe exponential growth when the atoms interact strongly with each other. As Fig. 4(d) shows, this is indeed the case. Detailed exploration of the interaction energy space shows that this analogy is rigorous (Fig. 5) and these three protocols are potentially equivalent to each other.

V. EQUIVALENCE OF CONTROL PROTOCOLS

The three protocols described here impose macroscopic control on the reaction kinetics through the rate constants. Although motivated by related physical intuitions, these ensembles of reaction graphs do differ in their microscopic

statistics, and it is important to ask whether they ultimately succeed in generating self-replicators for the same underlying topological reasons. Therefore, we sought to understand the modes of self-replication that each of these protocols employs. As Fig. 6 shows, the dominant modes of self-replication are, perhaps surprisingly, schemes 4 and 5, and schemes 1–3 are absent from all three protocols. Although surprising, this result is similar to those of previous experiments [10], where isolated ACCs were superseded by cooperative CCs as the main mode of self-replication. Furthermore, the equivalence between the three protocols indicates that the topology of the coupled-reaction network plays a more important role in determining the transient behavior than the rate constants.

To understand how the choice of the coupled-reaction graph may influence the transient growth behavior, we investigate the outcomes of protocol PF under various choices of the underlying coupled-reaction network. The analysis is described in detail in Appendixes C and D. Here, we describe the setup of the problem. Let us consider a reaction network with N reactions that are coupled with each other with probability p. Furthermore, let us assume that a fraction f_d of the N reactions is doubling reactions (reactions of the type $A + B \rightarrow 2C$). Then the number of two-step isolated ACCs (scheme 1) scales as

$$n_1 \sim (N - Nf_d)Nf_d p^2. \tag{4}$$

Similarly,

$$n_4 \sim \frac{1}{2}(N - Nf_d)^2 Nf_d p^4, \tag{5}$$

$$n_5 \sim \frac{1}{6}(N - Nf_d)^3 p^4. \tag{6}$$

It is easy to show from Eqs. (4)–(6) that n_1 is larger than n_4 if $p < \frac{\sqrt{2(1+f_d)}}{N}$, and n_1 is larger than n_5 if $p < \frac{\sqrt{6f_d(1+2f_d)}}{N}$. Both of these probabilities are incidentally lower than the average p for our system, which is roughly $\frac{2}{\sqrt{N}}$. Therefore, purely
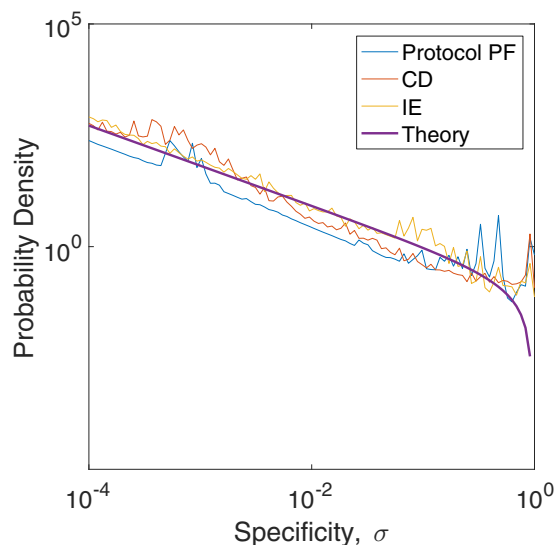
FIG. 7. PDF of specificity, σ, for three different protocols and a theoretical estimate assuming that the propensities are distributed as $\rho_p(x) \sim x^\nu \exp(-\lambda x)$. The plot corresponds to $\nu = -0.9$ and $\lambda = 0.01$. Despite the dissimilarity of the choice of rate constants, the specificity distribution is statistically identical in the three protocols.

by numbers, schemes 4 and 5 are more likely than schemes 1–3. However, as stated earlier, self-replication occurs only when the specificities of the reactions in a given motif satisfy the required conditions. For schemes 1–3, the specificity of the cycle has to be greater than 0.5 or, on average, the specificities of the reactions comprising the ACCs has to be greater than $\frac{1}{\sqrt{2}} \approx 0.71$. On the other hand, the conditions for schemes 4 and 5 are much more lenient, as verified by Table I. To estimate the likelihood of meeting these conditions, we estimate the probability distribution of the specificities (Appendix E). Under the assumption that the propensities for various reactions are distributed as $\rho_p(x) \sim x^\nu \exp(-\lambda x)$, the PDF of the specificity σ follows the distribution described in Fig. 7. It is evident from the PDF that one is hardly likely to find reactions with specificities higher than 0.71. On the other hand, one is quite likely to find reactions with specificities less than 0.5, which can satisfy the conditions required for schemes 4 and 5. Furthermore, despite the differences in the choice of rate constants the specificity distributions for the three protocols are statistically identical to the theoretical approximation. Therefore, the structural identity of the coupled-reaction graph as well as the statistical similarity of the specificity distribution is the origin of microscopic equivalence between the three protocols.

VI. DISCUSSION

In this paper, we have developed and investigated a model chemical system where the constituent chemicals interact with each other through stoichiometric reactions. We have solved this model under three protocols that impart different levels of macroscopic control over the rate constant distribution of the reactions. We have determined that despite the macroscopic differences, the microscopic kinetics responsible for self-replication is the same for all three protocols. In all three
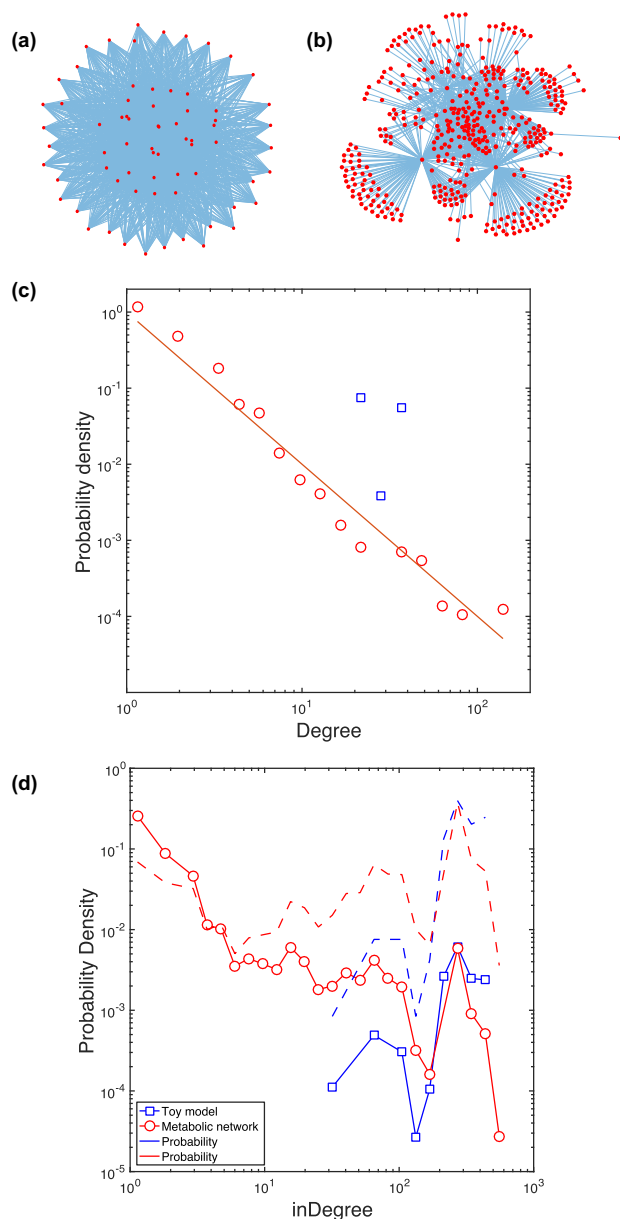

FIG. 8. Comparison of metabolic and toy chemical networks. A *reactant network* can be constructed by adding an undirected edge between two molecules if they react together in a reaction. In the network theory literature, this network has traditionally been referred to as the *reaction graph*. (a) Reactant graph of the toy chemical network considered here and (b) reactant graph of a metabolic network [23]. (c) The degree distribution of the reactant networks shows that the metabolic network is scale-free (red circles), whereas the toy chemical network has nearly the same degree for all the nodes (blue squares). In contrast, the *coupled-reaction network* is constructed by adding a directed edge between two reactions if the product of the first reaction is a reactant for the other. The coupled-reaction networks for the metabolic and the toy reaction networks are nearly identical and they look like the coupled-reaction graph shown in Fig. 2(b). (d) This observation is reflected in their in-degree distribution as well (the out-degree is similar). Although the PDFs are different for smaller in-degrees, they both have a peak at high in-degree values (solid lines with symbols). When translated to probabilities (dashed lines), both networks are dominated by nodes with high in-degrees, implying their potential functional similarities.

protocols, self-replication occurs due to the proliferation of coupled catalytic cycles and not due to isolated autocatalytic cycles, a result similar in spirit to that of an earlier experiment [10]. Furthermore, we have also shown that the criteria for self-replication from the proliferation of an isolated auto-catalytic cycle are very different from the criteria for the self-replication of coupled catalytic cycles. In fact, the cycle specificity, a well-known metric, can be much less than 0.5 and the molecules involved can still grow exponentially, in complete violation of the criteria established previously [4,5]. Although our criteria were developed in the context of a simple toy chemical system, the complexity of our model is comparable to that of metabolic networks. As shown in Fig. 8, although the reactant networks (see the figure for definition) are vastly different, the coupled-reaction networks are quite similar. Therefore, we argue that the criteria established here are applicable to real chemical networks as well.

In the light of the results described here, the future de-sign of self-replicating systems should focus on developing a chemical environment conducive for the proliferation of coupled catalytic cycles as opposed to isolated autocatalytic cycles, since the former can survive even when the reactions are not very specific. Creating such an environment through microscopic tuning of the rate constants is, by no means, easy. However, as we have shown here, it is possible to control coarse features of the chemical network, such as the width of the rate constant distribution and the interaction energies between the building blocks, to achieve the same goal easily.

Many factors may affect the viability of these design conditions. First, in this paper, we have chosen to report the behavior of the model in a regime in which the supply of resources is not a limiting factor. In simulations with limited resources, however, exponential growth can be hindered if the system reaches chemical equilibrium before the onset of exponential growth, consistent with previous studies [4,24]. Second, we have focused implicitly on the regime of a large and dilute reaction pot where mass-action kinetics applies. Of course, in any real reactor, the finite total number of particles would lead to small-number noisiness in the early emergence and growth of self-replicators that come about from bound states that are initially at a low concentration or totally ab-sent. This means that our results are most likely to apply in settings where the components feeding autocatalytic cycles are not themselves difficult to form rapidly from promiscuous reactions among components present in the initial condition. Finally, it is certain that topological quantities other than p_{fast} also can play an important role in determining the likelihood of self-replication. For example, the edge degree distribution of the coupled-reaction graph, which is nearly uniform here, is an important determinant of the reaction kinetics. However, for the purpose of clarity and brevity, we postpone this discus-sion for the future.

APPENDIX A: MATERIALS AND METHODS

1. Numerical solution of differential equations

We solved the systems of reactions assuming mass action kinetics. The concentrations of B and G were kept constant at 1, whereas the other molecules were initialized with con-centration 0. We solved the resultant systems of differential equations with ODE23tb, a stiff solver in MATLAB. The simulations were run until the system reached chemical equi-librium. Due to the stiffness of the differential equations, the solution sometimes failed to reach chemical equilibrium during the run time of the code, but it did not affect the growth regime. Hence, all the results reported here are unaffected by this limitation of the numerical algorithm.

2. Useful thermodynamic quantities

a. Propensity or rate: This is the product of the rate constant of a reaction and the concentration of the reactants raised to the appropriate power. For ex-ample, for the reaction $A + B -> C + D$ with rate con-stant k_+, and obeying mass action kinetics, the propensity is $k_+[A][B]$, where $[X]$ denotes the concentration of the reactant X.

b. Chemical current: Denoted J, this is the difference be-tween the propensities of the forward and reverse reactions of a reversible reaction. For example, for the reaction described earlier, $J = k_+[A][B] - k_-[C][D]$.

3. Specificity

Denoted σ here, the specificity is the ratio of the propensity of a given reaction to the sum of the propensities of all reactions that consume the resources required for the given reaction, including itself [4,5]. Mathematically, if π_i is the propensity of reaction i, then

$$\sigma = \frac{\pi_i}{\pi_i + \sum_{j \in \mathscr{C}} \pi_j}, \tag{A1}$$

where $\mathscr{C}$ is the set of all parasitic reactions that consume the resources required for reaction i. $C = |\mathscr{C}|$ is the number of such parasitic reactions. The cycle specificity is the product of the specificities of the reactions in the cycle.

In previous work [4,5], specificity was defined strictly for completely irreversible reactions. Therefore, its definition has to be modified for our system, where the reactions are reversible. We have found out that if the chemical current for a reaction is negative, it does not contribute to the calculation of the specificity. Therefore, to measure specificity, we have only used reactions whose chemical current is positive. Fur-thermore, often the concentrations of molecules span several orders of magnitude. Some of them may closely approach their equilibrium concentration long before other molecules. Under this condition, the concentrations of these molecules

are unaffected by the consumption of various reactions. As a result, we have ignored any parasitic reactions that consume these molecules from our calculation of specificity.

4. Growth exponent

At any given instant, t, the instantaneous growth rate of the concentration, $dc(t)/dt$, is a simple algebraic function of the concentration, $c(t)$. Formally,

$$\frac{dc}{dt} = rc^{\gamma}, \tag{A2}$$

where γ is the *growth exponent* and r is a proportionality constant. For exponential growth $\gamma = 1$, for power-law (subexponential) growth $0 < \gamma < 1$, and for linear growth $\gamma = 0$. When the concentration grows exponentially ($\gamma = 1$), r is equal to the exponential growth rate constant.

In a typical time series, γ varies with time. Therefore, to assess the occurrence of exponential growth, in this paper, we measure and report only the maximum value of γ over a time series, also referred to as γ. It is possible that the concentration of a molecule grows exponentially for a very short time, but in this paper we do not consider this self-replication. Because self-replication is characterized by persistent exponential growth, we call concentration growth exponential if and only if the concentration increases by a factor of 10 through exponential growth. Stated differently, if and only if $\gamma = 1$ over at least a decade of concentrations, then we call this growth exponential growth.

5. Estimate of p_{fast}

To estimate p_{fast}, we find the fraction of reactions whose propensities are within 10% of the propensities of the reaction with the fastest propensity. This is a heuristic definition and we have determined that the result does not change as long as it varies between 1% and 20%. For smaller values, the quantitative result changes, but the qualitative result remains the same.

6. Random sampling

We sampled 100 different configurations for each random activation barrier ensemble. To estimate p_{sr} in Fig. 5, we binned the scatterplot into different parameter values (c_d or p_{fast}). Any bins with fewer than five data points were ignored.

APPENDIX B: MODES OF SELF-REPLICATION

In this Appendix, we establish the criteria for self-replication for the schemes described in Fig. 3.

1. Scheme 1

We consider only the two-step cycle, as it is easier to solve analytically. Numerical investigation shows (not shown here) that the result follows for three-step and higher cycles as well.

Let us consider the following two reactions:

$$X \rightarrow Y, \tag{B1}$$

$$Y \rightarrow 2X. \tag{B2}$$
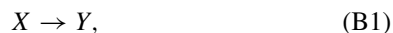
For simplicity we assume that these reactions are completely irreversible and have rate constants 1. We model the effect of parasitic side reactions by the annihilation reactions:

$$X \rightarrow \phi, \quad \text{rate constant} \quad r = k_x; \tag{B3}$$

$$Y \rightarrow \phi, \quad \text{rate constant} \quad r = k_y. \tag{B4}$$
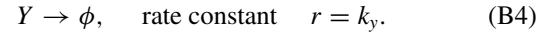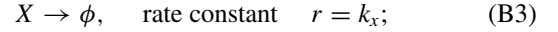
The Jacobian of these chemical systems is

$$J_1 = \begin{bmatrix} -(1 + k_x) & 2 \\ 1 & -(1 + k_y) \end{bmatrix}. \tag{B5}$$

One of the eigenvalues of this Jacobian has a positive real part if and only if

$$k_x + k_y + k_x k_y \leqslant 1. \tag{B6}$$

The specificities of the reactions are $\sigma_1 = 1/(1 + k_x)$ and $\sigma_2 = 1/(1 + k_y)$. Therefore, the cycle specificity is
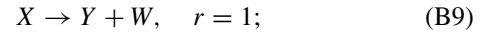
$$\sigma = \sigma_1 \times \sigma_2 \tag{B7}$$

$$= \frac{1}{1 + k_x + k_y + k_x k_y}. \tag{B8}$$

Therefore, for a positive eigenvalue, using $k_x + k_y + k_x k_y \leqslant 1$, we find that $\sigma \geqslant 0.5$, in agreement with previous results [4,5].

2. Schemes 2 and 3

The reactions are as follows:

$$X \rightarrow Y + W, \quad r = 1; \tag{B9}$$

$$Y \rightarrow \alpha X, \quad r = 1; \tag{B10}$$

$$W \rightarrow V, \quad r = 1; \tag{B11}$$

$$V \rightarrow 2W, \quad r = 1; \tag{B12}$$

$$X \rightarrow \phi, \quad r = k_x; \tag{B13}$$

$$Y \rightarrow \phi, \quad r = k_y; \tag{B14}$$

$$W \rightarrow \phi, \quad r = k_w; \tag{B15}$$

$$V \rightarrow \phi, \quad r = k_v. \tag{B16}$$

$\alpha = 1$ for scheme 2 and $\alpha = 2$ for scheme 3.

The corresponding Jacobian is

$$J_2 = \begin{bmatrix} -(1 + k_x) & \alpha & 0 & 0 \\ 1 & -(1 + k_y) & 0 & 0 \\ 1 & 0 & -(1 + k_w) & 2 \\ 0 & 0 & 1 & -(1 + k_v) \end{bmatrix}. \tag{B17}$$

J_2 can be solved similarly to J_1 and the criteria for positive eigenvalues are

$$k_w + k_v + k_w k_v \leqslant 1 \quad \text{for schemes 2 and 3, and} \tag{B18}$$

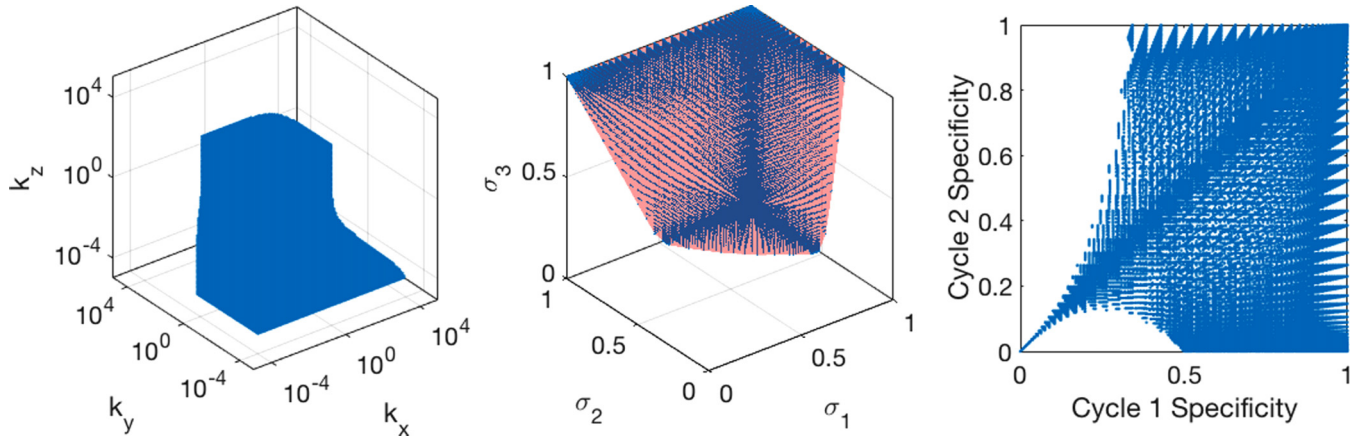$$k_x + k_y + k_x k_y \leqslant 1 \quad \text{only for scheme 3.} \tag{B19}$$
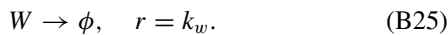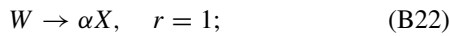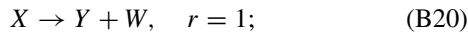
FIG. 9. Scheme 4. (Left) Scatterplot of $k_{x,y,w}$ values for which the real part of at least one eigenvalue is positive. (Center) Scatterplot of $\sigma_{1,2,3}$ for which the same condition is true. (Right) Scatterplot of cycle specificities of the two coupled cycles for the same condition. A positive eigenvalue is observed even when the cycle specificity is much below 0.5.

Therefore, the criterion for self-replication is the same as for scheme 1: the ACC specificity has to be greater than 0.5.

3. Schemes 4 and 5

The reactions are as follows:

$$X \rightarrow Y + W, \quad r = 1; \tag{B20}$$

$$Y \rightarrow X, \quad r = 1; \tag{B21}$$

$$W \rightarrow \alpha X, \quad r = 1; \tag{B22}$$

$$X \rightarrow \phi, \quad r = k_x; \tag{B23}$$

$$Y \rightarrow \phi, \quad r = k_y; \tag{B24}$$

$$W \rightarrow \phi, \quad r = k_w. \tag{B25}$$

$\alpha = 2$ for scheme 4 and $\alpha = 1$ for scheme 5.

The corresponding Jacobian is

$$J_3 = \begin{bmatrix} -(1 + k_x) & 1 & \alpha \\ 1 & -(1 + k_y) & 0 \\ 1 & 0 & -(1 + k_w) \end{bmatrix}. \tag{B26}$$

The eigenvalues of this Jacobian are complicated and finding criteria akin to those for schemes 1–3 is tiresome and impractical. However, the eigenvalues can be found numerically and as a function of $k_{x,y,w}$. In Fig. 9 and Fig. 10, we list the values of $k_{x,y,w}$ and the corresponding $\sigma_{1,2,3}$ for which the real part of at least one of the eigenvalues is positive. A positive eigenvalue, hence exponential growth, is observed even when the cycle specificity is less than 0.5.

APPENDIX C: PROBABILITY OF SELF-REPLICATION

For successful self-replication, there must be a region in the parameter space where driven autocatalytic cycles can proliferate without any interference from parasitic side reactions. Hence, it is helpful to understand the percolation
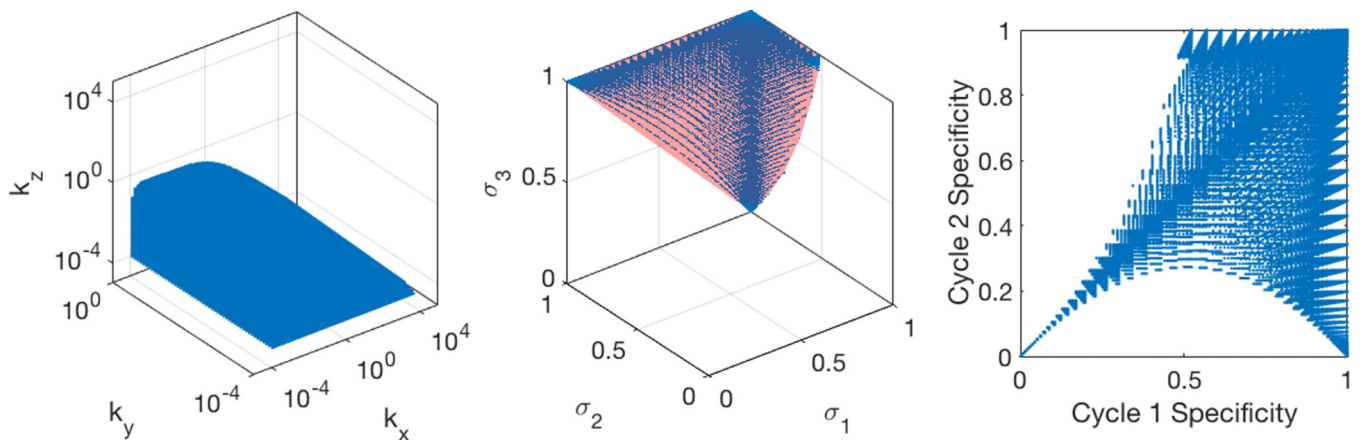

FIG. 10. Scheme 5. (Left) Scatterplot of $k_{x,y,w}$ values for which the real part of at least one eigenvalue is positive. (Center) Scatterplot of $\sigma_{1,2,3}$ values for which the same condition is true. (Right) Scatterplot of cycle specificities of the two coupled cycles for the same condition. A positive eigenvalue is observed even when the cycle specificity is much less than 0.5.

of autocatalytic cycles and the side reactions in our reaction network.

1. Percolation of autocatalytic cycles with access to food

The percolation of autocatalytic cycles with access to food depends on two factors:

(i) the availability of at least one autocatalytic cycle and

(ii) the availability of high-free-energy molecules to drive an autocatalytic cycle.

The probability of meeting both of these conditions is dependent on the underlying reaction network. However, a few qualitative features apply to any reaction network in general, which we outline here.

Let us assume that there are N total reversible reactions, half of which we designateforward reactions and the other half reverse. In a pruned reaction network, we sample reactions from the forward set with probability p_{ast} and include the corresponding reverse reaction as well. Therefore, there are, on average, $n_f = p_{fast}N$ reactions in the pruned reaction network. Let food, $\mathscr{F}$, be the molecules that are provided in abundance to fuel the chemical reactions. For example, in our model B and G are the fuel or food molecules and they can be used to produce other molecules required for various autocatalytic cycles.

a. Availability of food

Since we select the reactions randomly from the complete set of reactions, we are likely to encounter a situation where there are no mechanisms to utilize $\mathscr{F}$ in the pruned reaction network. Hence, we compute the probability of finding a mechanism to generate food from the fuel molecule in the pruned network. To do so, we note that there are two principal mechanisms for this conversion: (a) *direct reactions*, where two fuel molecules react to form a food molecule; and (b) *catalytic cycles*, where two or more fuel molecules are converted to food molecules via two or more coupled reactions. Let p_d be the probability of sampling a direct reaction and p_c be the probability of sampling a catalytic cycle. p_d can be easily approximated from the information about the reactions: if there are n_d direct reactions, then the probability of sampling one of them is $p_d = 2n_d/N$. The factor of 2 appears because either (a) we can choose all of the direct reactions to be forward reactions, in which case we sample n_d reactions from $N/2$ reactions, or (b) we pick their reverse reactions, automatically including them in the reaction network, hence we sample $2n_d$ reactions from N reactions. Calculating p_c is tougher.

The number of catalytic cycles increases with the number of constituent reactions m for $m \ll N$. However, a functional catalytic cycle requires a steady flow of flux through its constituent reactions to be effective. As pointed out in several studies [4,5], the likelihood of obtaining such functional cycles decreases exponentially in m for generic reaction networks. Hence, p_c can be well approximated by calculating the likelihood, $p_{c\mathscr{F}}$, of finding a two-step catalytic cycle that converts the fuels into food for the autocatalytic cycles. Generically, the reactions look like

$$\mathscr{F}_1 + \mathscr{C}_1 \rightarrow \mathscr{C}_2 + \mathscr{R}_1, \tag{C1}$$

$$\mathscr{F}_2 + \mathscr{C}_2 \rightarrow \mathscr{C}_1 + \mathscr{R}_2. \tag{C2}$$

Here, $\mathscr{F}_{1,2}$ are the fuel molecules and they can be identical; $\mathscr{C}_{1,2}$ are intermediate molecules that effectively act like catalysts; and $\mathscr{R}_{1,2}$ are the food molecules produced. The number of all two-step cycles, N_{C2}, can be calculated from the adjacency matrix of the reaction network. This number gives the probability of finding a catalytic cycle when two reactions that are not each other's reverse reaction are chosen randomly:

$$p_{cyc} = \frac{2N_{C2}}{N(N-2)}. \tag{C3}$$

With the additional information about the reactions that utilize $\mathscr{F}$, the number of such conversion cycles, $n_{c\mathscr{F}}$, can be computed, whence

$$p_{c\mathscr{F}} = n_{c\mathscr{F}}/N_{C2}. \tag{C4}$$

With these two probabilities, p_d and $p_{c\mathscr{F}}$, available, we compute the probability of finding at least one mechanism that converts fuel into food. To do so, we first compute the probability of finding at least one direct mechanism:

$$p_{d\geqslant 1} = 1 - \text{Prob(no direct mechanism)}$$
$$= 1 - (1 - p_d)^{n_f}. \tag{C5}$$

Similarly, the probability of finding at least one conversion cycle is

$$p_{c\mathscr{F}\geqslant 1} = 1 - \langle(1-p_{c\mathscr{F}})^{n_{C2}}\rangle \leqslant 1 - (1-p_{c\mathscr{F}})^{\langle n_{C2}\rangle} \tag{C6}$$

Here $\langle n_{C2}\rangle = p_{cyc} \times n_f(n_f - 2)/2$ is the expected number of cycles in the pruned network. Therefore, the probability of finding at least one mechanism of food production is

$$p_{food} = 1 - (1 - p_{d\geqslant 1})(1 - p_{c\geqslant 1}). \tag{C7}$$

b. Availability of autocatalytic cycles

Autocatalytic cycles are subsets of catalytic cycles. Hence, finding an autocatalytic cycle is harder than finding a catalytic cycle. Let us assume that there are n_{ac2} two-step autocatalytic cycles. Therefore, the probability that a randomly chosen catalytic cycle is an autocatalytic cycle is

$$p_{ac2} = n_{ac2}/N_{C2}. \tag{C8}$$

Therefore, the probability of finding at least one autocatalytic cycle is

$$p_{ac\geqslant 1} \leqslant 1 - (1 - p_{ac2})^{\langle n_{C2}\rangle}. \tag{C9}$$

Since this inequality provides an upper bound for $p_{ac\geqslant 1}$, for simplicity of calculation we assume that $p_{ac\geqslant 1} = 1 - (1 - p_{ac2})^{\langle n_{C2}\rangle}$. In the same spirit, we assume that $p_{c\mathscr{F}\geqslant 1} = 1 - (1 - p_{c\mathscr{F}})^{\langle n_{C2}\rangle}$.

c. Probability of autocatalytic cycles with access to food

Combining the results from the previous two sections, we find the probability of finding at least one autocatalytic cycle with access to food:

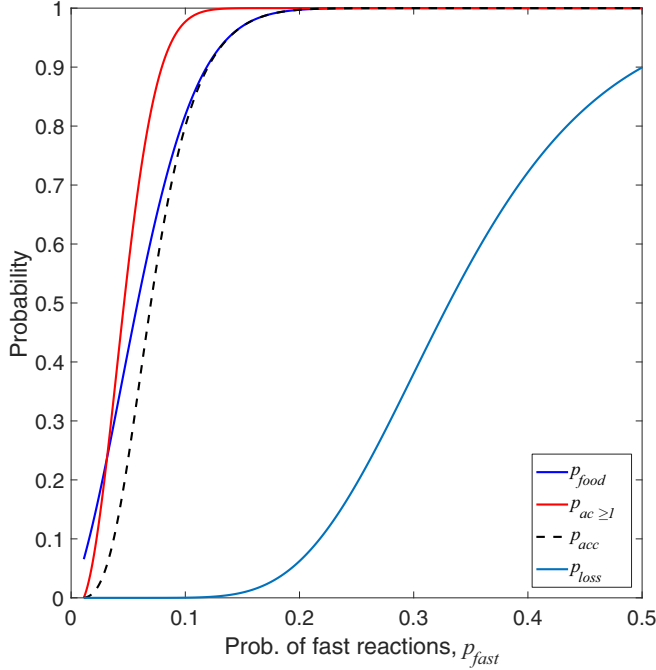$$p_{acc} = p_{ac\geqslant 1} \times p_{food}. \tag{C10}$$

FIG. 11. Percolation of various structures in the reaction network used vs the probability of fast reactions. Mechanisms that convert fuel into food, p_{food} (solid blue line); autocatalytic cycles, $p_{ac \geqslant 1}$ (solid red line); autocatalytic cycles with access to food, p_{acc} (dashed black line); and side reactions, p_{loss} (solid gray-blue line).
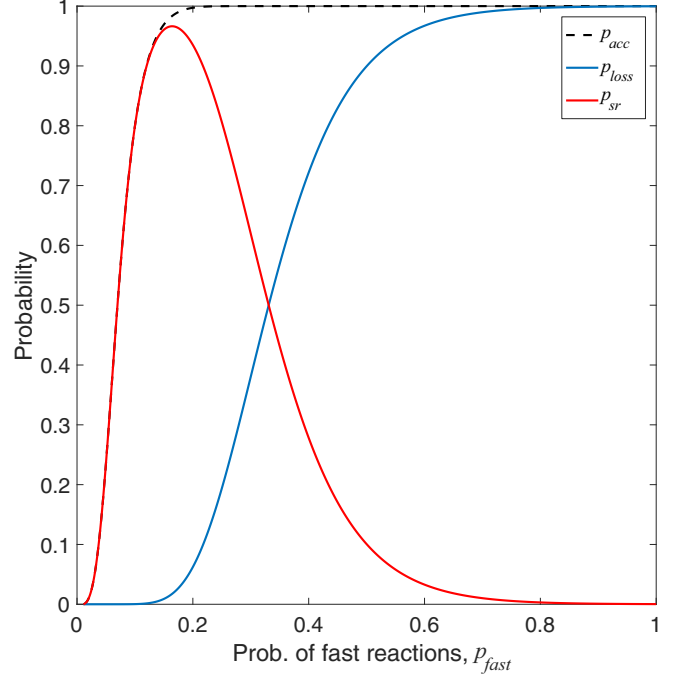

FIG. 12. Probability of self-replication vs probability of fast reactions. Probabilities of autocatalytic cycles with access to food, p_{acc} (dashed black line); side reactions, p_{loss} (solid gray-blue line); and self-replication, p_{sr} (solid red line).

2. Probability of side reactions

Let n_R be the average number of reactions that a particular molecule reacts in and $p_R = n_R/N$ be the average probability that a particular molecule is the reactant in a randomly chosen reaction. Hence, if n_f reactions are chosen randomly, then the probability that a molecule reacts in more than one reaction is

$$p_{r>1} = 1 - (1 - p_r)^{n_f} - n_f p_r (1 - p_r)^{n_f - 1}. \quad (C11)$$

Statistically, as long as there is at least one molecule that reacts in at most one reaction, there will be at least one autocatalytic cycle without any side reactions, which will permit exponential growth. Hence, side reactions start to interfere only when all the molecules take part in more than one reaction. The emergence of lossy side reactions also depends on whether or not dimerization reactions, such as $B + G \rightarrow BG$ and others, are forbidden. If one or more of them are forbidden, then the percolation of lossy side reactions becomes more difficult than when all of them are allowed. Therefore, the probability of finding all autocatalytic cycles with side reactions is

$$p_{loss} = \text{Prob(all molecules except fuels}$$
$$\times \text{ react in more than one reaction)}$$
$$= p_{r>1}^{N_M - N_{\mathscr{F}}} \times (1 - (1 - p_d)^{n_f}). \quad (C12)$$

Here p_d is the probability of a dimerization reaction, which is also the probability of direct access to the food. N_M is the total number of molecules in the reaction network and $N_{\mathscr{F}}$ is the number of fuel molecules.

3. Probability of self-replication

An autocatalytic cycle runs efficiently if it has direct access to available food and there are no lossy side reactions. Hence, the probability of observing self-replication is

$$p_{sr} = p_{acc} \times (1 - p_{loss}). \quad (C13)$$

4. Percolation probabilities and conditions for self-replication

As shown in Fig. 11, in the reaction network used in our model, the percolation of autocatalytic cycles with access to food occurs at a lower value of p_{fast} than the percolation of lossy side reactions. Hence, for some intermediate values of p_{fast}, we obtain a reaction network that is composed predominantly of interacting autocatalytic cycles with no side reactions. In this intermediate region, self-replication occurs optimally (Fig. 12). It is easy to imagine a reaction network where the opposite happens: p_{loss} percolates before p_{acc}. In the intermediate region the network is more treelike and in such a network self-replication is unlikely to happen. Therefore, *in general, if a cycle is the predominant structural motif in a reaction network, then it is conducive for self-replication.*

5. Asymptotic bound on the probability of self-replication

When $N_m \rightarrow \infty$ and $p_r \rightarrow 0$ ($N \rightarrow \infty$), p_{loss} is a step function and provides a strong upper bound for p_{fast} values that allow self-replication. This upper bound can be calculated by finding the p_{fast} value for which the derivative of p_{loss} with respect to p_{fast} is maximum. Upon calculation, we find that for
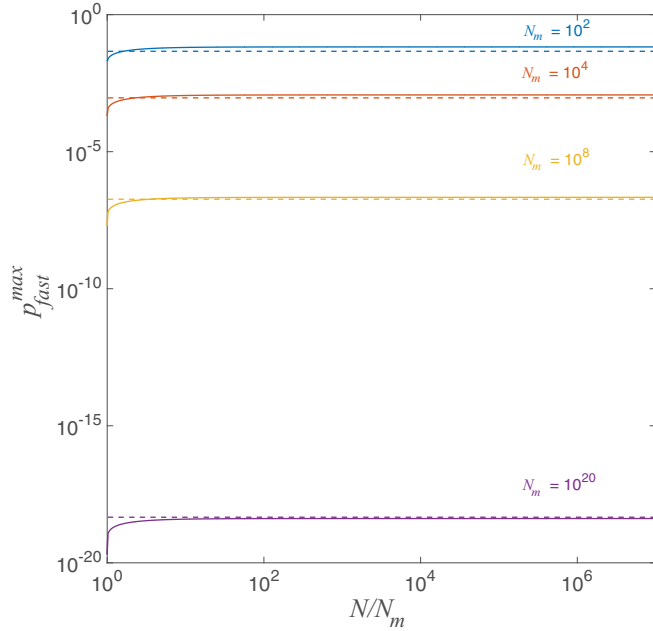
FIG. 13. Position of the maximum, $p_{\text{fast}}^{\max}$, vs complexity of the reaction network, N/N_m. Irrespective of the value of N_m, $p_{\text{fast}}^{\max}$ remains unchanged when the complexity N/N_m is large enough ($\geqslant 10$) as shown in the numerically calculated curves (solid lines). In the large-complexity limit, when N_m is large, $p_{\text{fast}}^{\max}$ is well approximated by the theoretical bound (dashed lines) in Eq. (C14).

self-replication to occur,

$$\boxed{p_{\text{fast}}^{\max} \leqslant \frac{\log N_m}{N_m}}. \tag{C14}$$

Variation of $p_{\text{fast}}^{\max}$ for some values of N_m is shown in Fig. 13.

6. Factors affecting the probability of self-replication

It is unlikely that p_{fast}, which controls the mean number of nodes in the reaction network, is the only factor that determines the probability of self-replication. In any network, the most important network elements are the number of nodes, number of edges, and number of cycles, which we measure, respectively, by the number of fast reactions n_f, mean degree of the nodes in the reaction network n_e, and number of two cycles in the reaction network $n_{\text{ac}2}$. In any graph these three quantities are linearly dependent on each other. Therefore, we have chosen to report the dependence of exponential growth on p_{fast} and n_e. We find that an optimal p_{fast} is preferred for exponential growth, but there is no such preference for subexponential growth (Fig. 14). In contrast, n_e has a different variance but the same mean for exponential and subexponential growth, implying that n_e is not a determinant of exponential growth.

APPENDIX D: CONTROL OF p_{sr} THROUGH DIMERIZATION REACTIONS

The relation $p_{\text{sr}} = p_{\text{acc}} \times p_{\text{loss}}$ is purely topological, in the sense that both p_{acc} and p_{loss} depend only on the reaction network properties. Therefore, by controlling these proper-
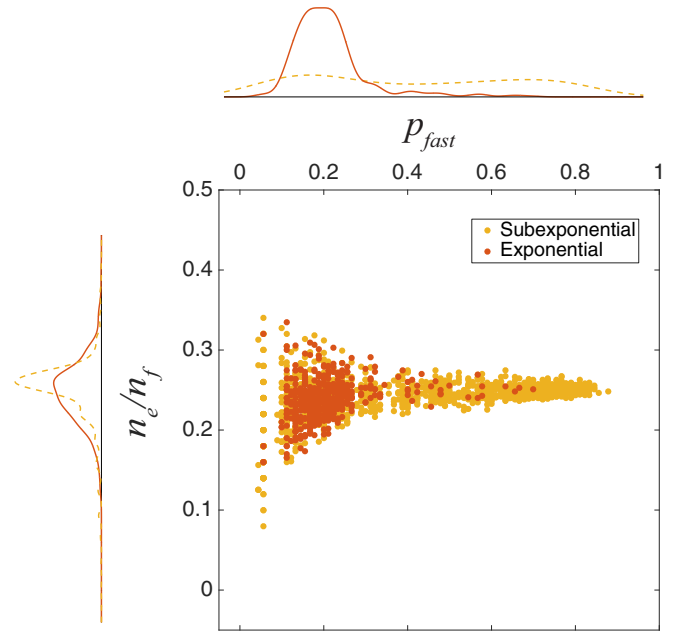

FIG. 14. Scatterplot of the mean degree per node, n_e/n_f, and p_{fast}. Red points correspond to exponential growth and orange points correspond to subexponential growth. The histogram on the y axis shows that the emergence of exponential growth does not have a strong dependence on the mean degree distribution.

ties, such as the density of autocatalytic cycles, the degree distribution, and the number of reactions, it is possible to control the range of p_{fast} over which p_{sr} remains reasonably high. The density of the autocatalytic cycles is difficult to control independently since in a strongly interacting network, such as ours, they are too numerous and interdependent, which renders the control of p_{acc} nearly impossible. On the other
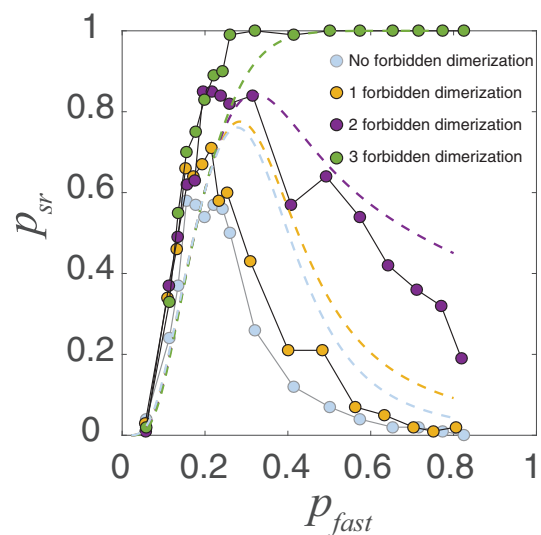

FIG. 15. Probability of self-replication vs probability of fast reactions with different numbers of forbidden dimerization reactions. Increasing the number of forbidden dimerization reactions increases the stability of the food molecules B and G, and the probability of self-replication increases.

hand, there is a simple way to control p_{loss}. The lossy side reactions overwhelm the autocatalytic cycle if the reaction network is sufficiently "well connected," i.e., if it is possible to generate all the molecules by seeding the reaction network with the atoms (B and G) only. Therefore, dimerization reactions—reactions that convert the atoms to their dimers—are necessary to construct a well-connected reaction network and, hence, the percolation of lossy side reactions. Consequently, by manipulating the rate of the dimerization reactions, the percolation of p_{loss} can be manipulated. As we show in Fig. 15, rendering one or more dimerization reactions always forbidden improves the probability of self-replication. In fact, when all three of them are always forbidden, for large p_{fast}, self-replication occurs with unit probability. The propensity of the dimerization reactions determines the stability of the food molecules, B and G. Therefore, in general, this result implies that the more stable the food molecule, the more likely it is to attain exponential growth.

APPENDIX E: PROBABILITY DISTRIBUTION FOR SPECIFICITY

Let us assume that the propensities (rates), x, are distributed according to the probability distribution function $\rho_p(x)$. Let us further assume that every reaction competes, on average, with C other reactions. In reality, each reaction competes with a varying number of reactions, but for this example, we ignore that complication. Furthermore, let us assume that these reactions, on average, have propensity μ, which is the mean propensity. Therefore, on average, a reaction with propensity x will have specificity

$$\sigma = \frac{x}{x + C\mu}. \tag{E1}$$

The probability distribution for σ is then obtained by a change of variables:

$$\rho_s(\sigma)d\sigma = \rho_p(x)dx, \tag{E2}$$

$$\therefore \rho_s(\sigma) = \rho_p\left(\frac{C\mu\sigma}{1-\sigma}\right) \times \frac{(1-\sigma)^2}{C\mu}. \tag{E3}$$

For exponentially distributed propensities, $\rho_p(x) = \lambda \exp(-\lambda x)$, where $\mu = 1/\lambda$:

$$\rho_s\sigma = \frac{\lambda^2}{C}(1-\sigma)^2 \exp\left(-\frac{C\sigma}{1-\sigma}\right). \tag{E4}$$

For power-law-distributed propensities with exponential cutoff $\rho_p(x) \sim x^\nu \exp(-\lambda x)$, where $\mu = \frac{\nu+1}{\lambda}$,

$$\rho_s(\sigma) \sim \left(\frac{\Gamma(\nu+1)}{\lambda^{\nu+1}}\right)^{\nu+1} \left(\frac{C\sigma}{1-\sigma}\right)^\nu$$
$$\times \exp\left(-\frac{\Gamma(\nu+1)}{\lambda^{\nu+1}}\frac{C\lambda\sigma}{1-\sigma}\right). \tag{E5}$$

[1] A. Butlerow, C.R. Acad. Sci. **53**, 145 (1861).

[2] R. Breslow, Tetrahedron Lett. **1**, 22 (1959).

[3] F. J. Dyson, J. Mol. Evol. **18**, 344 (1982).

[4] E. Szathmáry, Philos. Trans. R. Soc. London B **361**, 1761 (2006).

[5] G. King, Biosystems **15**, 89 (1982).

[6] A. J. Bissette and S. P. Fletcher, Angewandte Chem. Int. Ed. **52**, 12800 (2013).

[7] N. Paul and G. F. Joyce, Curr. Opin. Chem. Biol. **8**, 634 (2004).

[8] J. M. Carnall, C. A. Waudby, A. M. Belenguer, M. C. Stuart, J. J.-P. Peyralans, and S. Otto, Science **327**, 1502 (2010).

[9] T. Wang, R. Sha, R. Dreyfus, M. E. Leunissen, C. Maass, D. J. Pine, P. M. Chaikin, and N. C. Seeman, Nature **478**, 225 (2011).

[10] N. Vaidya, M. L. Manapat, I. A. Chen, R. Xulvi-Brunet, E. J. Hayden, and N. Lehman, Nature **491**, 72 (2012).

[11] Z. Zeravcic and M. P. Brenner, Proc. Natl. Acad. Sci. USA **111**, 1748 (2014).

[12] J. W. Sadownik, E. Mattia, P. Nowak, and S. Otto, Nat. Chem. **8**, 264 (2016).

[13] A. Šarić, A. K. Buell, G. Meisl, T. C. Michaels, C. M. Dobson, S. Linse, T. P. Knowles, and D. Frenkel, Nat. Phys. **12**, 874 (2016).

[14] U. Barenholz, D. Davidi, E. Reznik, Y. Bar-On, N. Antonovsky, E. Noor, and R. Milo, eLife **6**, e20667 (2017).

[15] D. Zwicker, R. Seyboldt, C. A. Weber, A. A. Hyman, and F. Jülicher, Nat. Phys. **13**, 408 (2017).

[16] J. L. England, J. Chem. Phys. **139**, 121923 (2013).

[17] N. Perunov, R. A. Marsland, and J. L. England, Phys. Rev. X **6**, 021036 (2016).

[18] S. A. Kauffman, J. Theor. Biol. **119**, 1 (1986).

[19] S. Jain and S. Krishna, Proc. Natl. Acad. Sci. USA **98**, 543 (2001).

[20] Z. Zeravcic and M. P. Brenner, Proc. Natl. Acad. Sci. USA **114**, 4342 (2017).

[21] Y. Wang, Y. Wang, D. R. Breed, V. N. Manoharan, L. Feng, A. D. Hollingsworth, M. Weck, and D. J. Pine, Nature **491**, 51 (2012).

[22] R. Zhang, J. M. Dempster, and M. O. de la Cruz, Soft Matter **10**, 1315 (2014).

[23] J. E. Goldford, H. Hartman, R. Marsland, and D. Segre, bioRxiv (2018), https://www.biorxiv.org/content/early/2018/12/04/487660.full.pdf.

[24] D. Sievers and G. Von Kiedrowski, Nature **369**, 221 (1994).